MPMI Vol. 26, No. 4, 2013, pp. 379–386. http://dx.doi.org/10.1094/MPMI-08-12-0207-R.

e-Xtra*

Phytoplasma-Triggered Ca^{2+} Influx Is Involved in Sieve-Tube Blockage

Rita Musetti,[1] Stefanie V. Buxa,[2] Federica De Marco,[1] Alberto Loschi,[1] Rachele Polizzotto,[1] Karl-Heinz Kogel,[1] and Aart J. E. van Bel[2]

[1]Department of Agricultural and Environmental Sciences, University of Udine, via delle Scienze, 208, I-33100 Udine, Italy; [2]Department of Phytopathology and Applied Zoology, Justus Liebig University, Heinrich-Buff-Ring 26-32, D-35392 Giessen, Germany

Submitted 31 August 2012. Accepted 30 November 2012.

Phytoplasmas are obligate, phloem-restricted phytopathogens that are disseminated by phloem-sap-sucking insects. Phytoplasma infection severely impairs assimilate translocation in host plants and might be responsible for massive changes in phloem physiology. Methods to study phytoplasma-induced changes thus far provoked massive, native occlusion artifacts in sieve tubes. Hence, phytoplasma-phloem relationships were investigated here in intact *Vicia faba* host plants using a set of vital fluorescent probes and confocal laser-scanning microscopy. We focused on the effects of phytoplasma infection on phloem mass-flow performance and evaluated whether phytoplasmas induce sieve-plate occlusion. Apparently, phytoplasma infection brings about Ca^{2+} influx into sieve tubes, leading to sieve-plate occlusion by callose deposition or protein plugging. In addition, Ca^{2+} influx may confer cell wall thickening of conducting elements. In conclusion, phytoplasma effectors may cause gating of sieve-element Ca^{2+} channels leading to sieve-tube occlusion with presumptive dramatic effects on phytoplasma spread and photoassimilate distribution.

Phytoplasmas are prokaryotic microorganisms that bring about several hundred diseases affecting economically important crops such as ornamentals, vegetables, fruit trees, and grapevines. Phytoplasmas mostly colonize the sieve tubes and manipulate the host to ensure an efficient distribution and multiplication (Hogenhout et al. 2008). To date, the physiological relationship between phytoplasmas and their hosts has remained largely unexplored (Hogenhout et al. 2008). Phytoplasmas have a very small genome (530 to 1,350 kb) and lack many genes otherwise considered to be essential for cell metabolism (Marcone et al. 1999).

Several studies demonstrated that phytoplasma infection induces important cytological and physiological modifications in the phloem of host plants, in several cases severely affecting phloem transport (Braun and Sinclair 1978; Kartte and Seemüller 1991; Lepka et al. 1999; Maust et al. 2003). It has been speculated that mechanisms involved in phloem impairment could differ between pathosystems and vary with the plant susceptibility to infection (Kartte and Seemüller 1991; Musetti and Favali 1999).

Histological studies on several plant species infected by phytoplasmas showed that the first detectable anatomical aberration is an abnormal deposition of callose in the sieve-plate regions which is followed by a collapse of sieve elements and companion cells (Kartte and Seemüller 1991). Sieve-plate occlusion has been regarded as a defense mechanism leading to the formation of physical barriers aimed to achieve pathogen containment (Musetti et al. 2008). In phytoplasma-infected tobacco plants treated with fungal elicitors (Lherminier et al. 2003) as well as in other pathosystems (Elad and Evensen 1995; Koh et al. 2012), concomitant callose accumulation and P protein agglutination have been reported to occur in sieve tubes in response to infection.

Expression of genes responsible for callose deposition in sieve tubes is finely tuned. This is exemplified by the role of callose synthase (CLS7) in normal sieve-element maturation in *Arabidopsis* as well as in the response to wounding (Barratt et al. 2011; Xie et al. 2011), showing that callose production is a balancing act for plants. An analogous trade-off event must occur in infected plants: massive callose deposition restricts host colonization by phytoplasmas but, at the same time, impedes photo-assimilate transport. Moreover, recovery—a spontaneous reduction of the disease symptoms of phytoplasma-infected plants—is accompanied by an appreciable upregulation of two callose synthase and three phloem protein (PP2) genes (Musetti et al. 2010).

It has been demonstrated that sieve plates are plugged by proteins in response to mechanical injuries prior to callose deposition (Furch et al. 2007, 2010). Structural proteins in sieve tubes have been observed for a long time (Cronshaw and Sabnis 1990). Some of these proteins (later named sieve-element occlusion [SEO] proteins) (Pelissier et al. 2008) are involved in sieve-tube plugging. In members of the family Fabaceae, SEO are aggregated in giant protein bodies called forisomes (Knoblauch et al. 2001). In response to different stresses (wounding, burning, and cold), forisomes undergo a conformational change from a condensed to a dispersed state which plugs the sieve plates and prevents loss of photoassimilates (Furch et al. 2007; Knoblauch et al. 2001; Thorpe et al. 2010). Genes encoding SEO protein components do not occur only in Fabaceae species (Pelissier et al. 2008; Tuteja et al. 2010) but appear to be widespread among dicotyledonous plants such as apple, grapevine, and *Arabidopsis* (Rüping et al. 2010). Preliminary gene expression analyses for SEO protein components revealed an upregulation in phytoplasma-infected apple trees compared with healthy ones (Musetti et

Corresponding author: R. Musetti; Telephone: +(39) 0432 558521; Fax: +(39) 0432 558501; E-mail: Rita.Musetti@uniud.it

*The *e*-Xtra logo stands for "electronic extra" and indicates that a supplementary table is published online.

al. 2011), indicating potential involvement in response to phytoplasma infection.

Callose synthesis as well as P protein aggregation are Ca^{2+}-dependent phenomena (Knoblauch et al. 2001; Köhle et al. 1985) triggered by Ca^{2+} influx into sieve elements (Furch et al. 2007, 2009, 2010). Thus, occlusion events suggest that phytoplasma infection induces gating of Ca^{2+} channels and consequent influx of Ca^{2+} into sieve elements (Musetti et al. 2008). This would confer a quick and straightforward defense response in plants undergoing phytoplasma attack.

Because unequivocal in vivo evidence for phytoplasma-mediated sieve-tube occlusion is lacking thus far, the aim of this work was to design and optimize a method to perform in vivo observation of the phloem in phytoplasma-infected intact plants. Deposition of callose and changes in forisome conformation were examined in relation to mass flow and compared between healthy and phytoplasma-infected broadbean (*Vicia faba* L.) plants (used as hosts of '*Candidatus* Phytoplasma vitis', associated with grapevine Flavescence Dorée [FD]) by using confocal laser-scanning microscopy (CLSM). In particular, we evaluated whether phytoplasmas induce Ca^{2+} influx leading to occlusion by callose deposition or protein plugging and inherent impairment of mass flow.

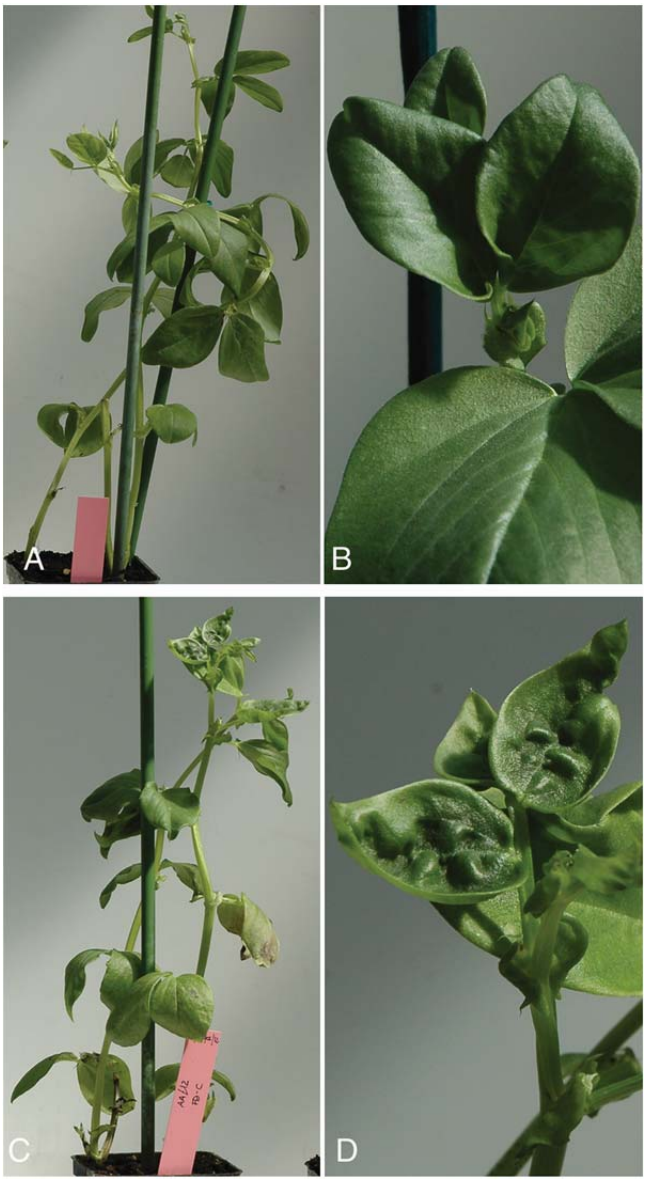

Fig. 1. Images of healthy (left half of the panel) and Flavescence Dorée (FD)-infected (right half) *Vicia faba* plants. **A** through **D,** Whole plants and leaf details. **A** and **B,** Healthy *V. faba* plants show regular growth and do not develop disease symptoms. **C** and **D,** In FD-infected plants (C and D) typical symptoms are visible, such as general decline, beginning leaf decoloration, and leaf deformation.

RESULTS

Plant materials and phytoplasma detection by polymerase chain reaction.

Control *V. faba* plants, not exposed to leafhoppers, showed regular growth without disease symptoms (Fig. 1A and B). In infected plants, typical FD symptoms such as leaf-size reduction, leaf yellowing, and curling (Fig. 1C and D) emerged approximately 1 month after inoculation by the insect vectors.

Real-time polymerase chain reaction (RT-PCR) of '*Ca.* P. vitis' 16SrRNA confirmed the presence of phytoplasmas in infected *V. faba* leaf samples before CLSM examination. Starting from 40 ng of total DNA, FD-phytoplasma 16SrDNA was detected in symptomatic samples, whereas no amplification of the 16SrRNA gene was obtained in healthy ones. DNAs isolated from FD-diseased *Catharanthus roseus* and FD-infected *Vitis vinifera* were also amplified as positive parallel controls (Supplementary Table S1).

Optical phytoplasma detection and mass flow.

In vivo observation of *Vicia faba* phloem by CLSM enabled us to observe sieve elements in intact plants. Under transmission light, healthy sieve elements were characterized by the presence of condensed forisomes (Fig. 2A), while the sieve plates were free of visible occluding substances (Fig. 2A).

After (5)6 carboxyfluorescein diacetate (CFDA) application to healthy *V. faba* plants, phloem-mobile (5)6 carboxyfluorescein (CF) was translocated through the sieve tubes and accumulated in the companion cells, which indicates a regular mass flow and a high degree of metabolic activity in companion cells (Fig. 2B). As reported previously for other cell types (Goodwin et al. 1990), CF accumulated in the vacuoles of phloem parenchyma cells. In stained sieve elements, several parietal plastids were visible (Fig. 2B), probably anchored to the plasma membrane (Ehlers et al. 2000). Nuclei were recognizable in both companion and phloem parenchyma cells (Fig. 2B), probably after CFDA movement through plasmodesmata. It was more difficult to focus and discern sieve tubes in FD-diseased plants due to the presence of thicker cell walls and sediments onto the sieve plates (Fig. 2C). In such plants, only a few sieve elements were weakly fluorescent after CFDA application, indicating that mass flow was blocked or strongly reduced (Fig. 2D). Even when mass flow in sieve tubes appeared to be reduced or eliminated, CFDA was observed to accumulate in the vacuoles of companion cells (Fig. 2D), which may indicate the maintenance of some metabolic ability.

After 4′,6-diamidino-2-phenylindole (DAPI) application to enable phytoplasma detection, no DAPI fluorescence showed up in sieve elements of healthy plants; only the nuclei of companion cells and phloem parenchyma cells were stained (Fig. 2E). Under transmission light, the sieve elements were well preserved and unstained in healthy plants (Fig. 2F). In FD-diseased plants, dotted fluorescent aggregates were accumulated predominantly at the sieve plates (Fig. 2G, arrows). In FD-diseased sieve elements, cell walls and sediments on the sieve plates were thicker than in control plants (Fig. 2H), as described above.

Successive local DAPI and distant CFDA staining demonstrated that absence of DAPI staining is related to intense CFDA translocation in the phloem of healthy plants (Fig. 2I and J). By contrast, DAPI fluorescence (Fig. 2K) coincides with

impaired sieve-tube translocation in infected plants (Fig. 2L). In both healthy and infected plants, the reverse CFDA/DAPI double-staining procedure produced results similar to those for DAPI/CFDA staining (Fig. 2M through P).

Occlusion events and Ca^{2+} concentration.

Combined 5-chloromethyl-fluoresceindiacetate and 5-chloromethyl-eosin-diacetate (CMFDA/CMFDA) staining provided unequivocal information on the forisome conformation and protein distribution inside the sieve elements of healthy and FD-diseased plants in CLSM images. In healthy plants, forisomes were always in the condensed, spindle-shaped form (Fig. 3A and B) and were mostly located near the sieve plates at the downstream end of the sieve elements. In FD-diseased plants, discrete forisomes were not detectable (Fig. 3C and D), which is indicative of their dispersion (Knoblauch et al. 2001). Unidentified protein structures—dispersed forisomes or clogged P proteins—occurred in FD-diseased sieve elements (Fig. 3C).

Aniline blue at nonlethal concentrations (Furch et al. 2007) was administered to bare-lying phloem tissue to acquire a qualitative in vivo estimate of callose deposition in sieve elements. In healthy plants, callose was not detectable (Fig. 3E) or occurred in minor amounts at the margins of the sieve plates (Fig. 3I) and the sieve elements were well preserved, containing condensed forisomes (Fig. 3F and J).

By contrast, aniline blue signals were much stronger in FD-diseased *V. faba* plants, indicating massive callose depositions at the sieve plates and along the sieve elements, probably at the pore-plasmodesmata-unit orifices (Fig. 3G) (Furch et al. 2009) to the point of plug formation (Fig. 3K, arrows). Increased thickness of the sieve-element walls and accumulation of dark material at the sieve plates were also visible under transmission light (Fig. 3H and L).

Oregon Green 1,2-bis(o-aminophenoxy)ethane-N,N,-N′,N′-tetraacetic acid (OGB-1) was used as a qualitative indicator of Ca^{2+} concentration inside the sieve elements. No fluorescent signals were detected in intact sieve elements of uninfected

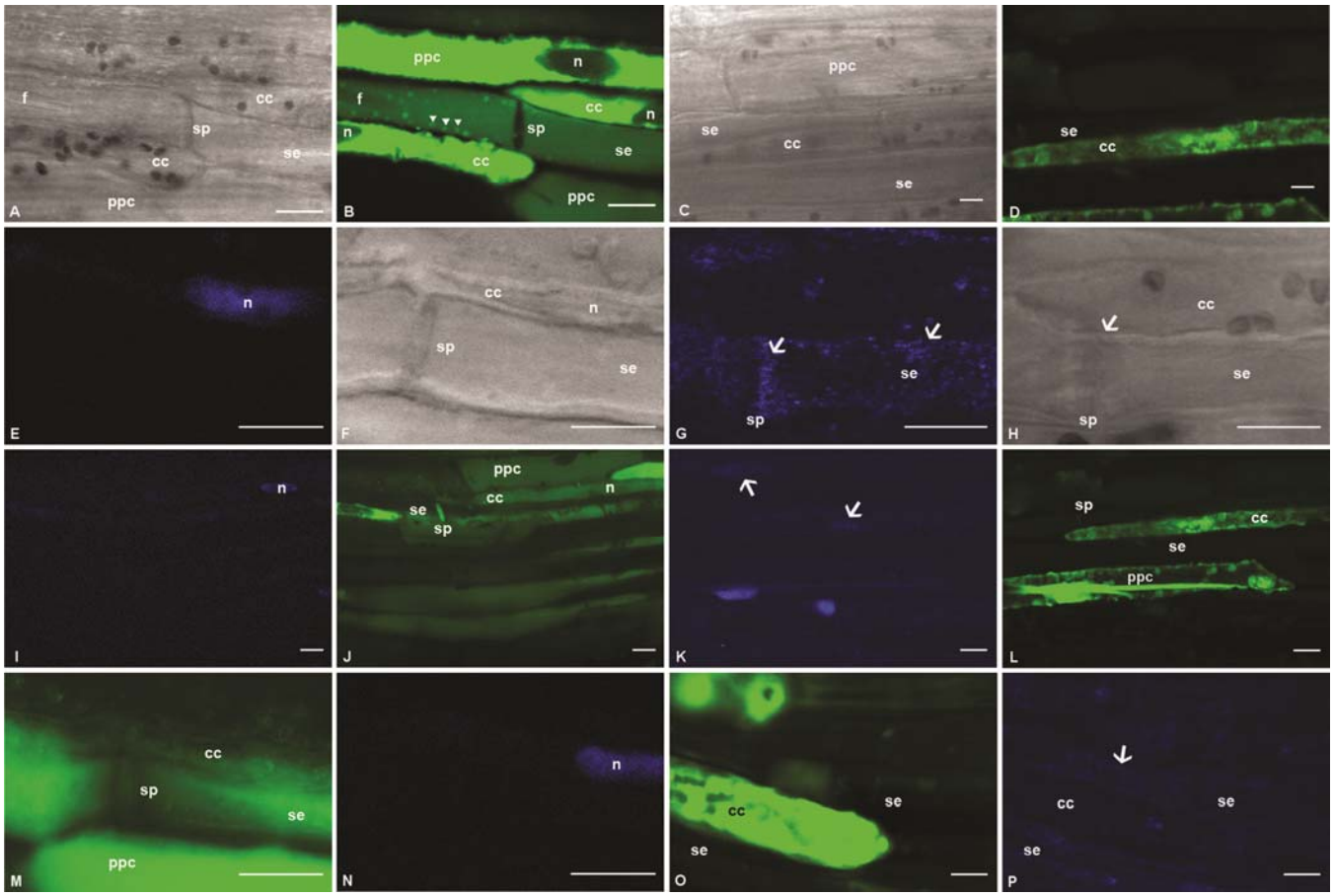

Fig. 2. Confocal laser-scanning microscopy (CLSM) images of phloem tissue in intact healthy (left half of the panel) and Flavescence Dorée (FD)-infected (right half) *Vicia faba* plants. **A** and **B,** Healthy and **C** and **D,** FD-infected phloem under **A** and **C,** transmission light and **B** and **D,** after distant (5)6 carboxyfluorescein diacetate (CFDA) application, observed at 488 nm. In healthy *V.* faba plants, sieve elements (se) are characterized by the presence of forisomes (A, f) and plastids (B, arrowheads). FD-infected *V. faba* plants do not show remarkable content in transmission light (C). Following sieve-tube translocation of CFDA in healthy plants (B), CFDA is accumulated in the vacuoles of companion (cc) and phloem parenchyma cells (ppc). With the exception of the vacuoles of companion cell (cc), fluorescence is absent in sieve elements of FD-infected plants (D), indicative of mass-flow inhibition. **E** and **F,** Healthy and **G** and **H,** FD-infected phloem after 4′,6-diamidino-2-phenylindole (DAPI) staining, observed at **E** and **G,** 405 nm and **F** and **H,** under transmission light. In sieve elements of FD-infected plants, blue fluorescent dots (arrows) mainly aggregate on both sides of the sieve plate (G, sp). Phloem in healthy plants remains unlabeled apart from the stained nuclei (E, n). Under transmission light, in healthy plants (F), cell walls and sieve plate thickening seem inconspicuous. Note the distorted thickened cell walls and sieve plate thickenings (arrow) visible in FD-infected plants (H). **I** through **L,** Subsequent local DAPI staining and distant CFDA application demonstrate that absence of DAPI staining (I) (apart from the stained nuclei) concurs with regular CFDA translocation (J) in the phloem of healthy plants. By contrast, DAPI fluorescence, indicating phytoplasma presence (K, arrows), seems to coincide with impaired sieve-tube translocation in infected plants (L). **M** through **P,** Reverse CFDA/DAPI double-staining procedure renders results similar to those obtained with DAPI/CFDA treatment in both healthy (M and N) and infected (O and P) plants. cc = companion cell, f = forisome, n = nucleus, ppc = phloem parenchyma cell, se = sieve element, sp = sieve plate. Arrowheads in B indicate sieve-element plastids; in G, K, and P, arrows indicate phytoplasma/DAPI fluorescence. Bars correspond to 10 µm.

V. faba plants (Fig. 4A). The identical optical section observed under transmission light showed unstressed sieve elements as inferred by the presence of condensed forisomes (Fig. 4B). In the phloem of diseased plants, OGB-1 fluorescence was often intense, with strong signals at the sieve plates (Fig. 4C and G). Under transmission light, condensed forisomes did not occur (Fig. 4D and H). Weak OGB-1 signals were sometimes found in healthy sieve elements (Fig. 4E, arrow) that were mechanically stressed as a result of the preparation procedure, as indicated by forisome dispersion (Fig. 4F).

Fluorescence was not detected in unstained healthy (Fig. 4I and J) or FD-infected (Fig. 4K and L) samples, with the exception of the chloroplasts. Neither of the excitation wavelengths used for the respective fluorochromes (405 nm [Fig. 4I and K] or 488 nm [Fig. 4J and L]) elicited fluorescent signals.

DISCUSSION

Because phytoplasmas are obligate parasites transmitted to host plants by insect vectors in a persistent manner (Hogenhout et al. 2008) and insect inoculation requires several days, it is difficult to pinpoint the exact moment at which phytoplasmas initiate the infective processes in host plants. Therefore, we were urged to use systemically infected plants to study occlusion events; however, it is obvious that the initial occlusion stages have not been caught here.

In vivo phytoplasma detection.

In contrast to the progress made in detection and taxonomic classification of phytoplasmas, very little is known about plant–phytoplasma interactions. Phytoplasmas induce characteristic symptoms in host plants, many of which (such as low productivity, stunting, general decline, and reduced vigor) point to impairment of sieve-tube function (Kartte and Seemüller 1991). Because phytoplasmas (mainly in the case of woody plants) are not evenly distributed over the sieve tubes (Faoro 2005), despite the systemic spread via the phloem, phloem impairment and the subsequent development of the disease symptoms cannot be explained solely by the presence of phytoplasmas plugging the sieve elements, but also must involve the impact of phytoplasma-secreted effector proteins on plant cells (Hogenhout et al. 2008).

Knowledge about the phytoplasma capability to spread through sieve elements is essential for understanding the relationships with the host. Previous attempts to describe the colonization behavior of phytoplasmas via sieve tubes have been made using conventional microscopic, serological, or molecular methods (Lherminier et al. 1994; Marcone 2010). Cytological modifications such as sieve-element necrosis, abnormal callose deposition at the sieve plates, sieve-element wall thickening, and starch accumulation in the shoots of susceptible plants have been documented by electron microscopic observations (Braun and Sinclair 1978; Kartte and Seemüller 1991; Musetti and Favali 1999; Musetti et al. 1994).

Moreover, one should bear in mind that studies of ultrathin sections are laborious and time-consuming and only small portions of fixed and embedded tissue of interest can be examined. Both electron-microscopic techniques and molecular methods, based on extraction of different cell components (i.e., DNA, RNA, and proteins), are destructive. The necessity to kill plant tissues causes instantaneous, irreversible, and massive reactions of sieve elements to wounding (van Bel 2003), which may lead to pieces of misleading information and erroneous interpretations. To intercept this drawback, Christensen

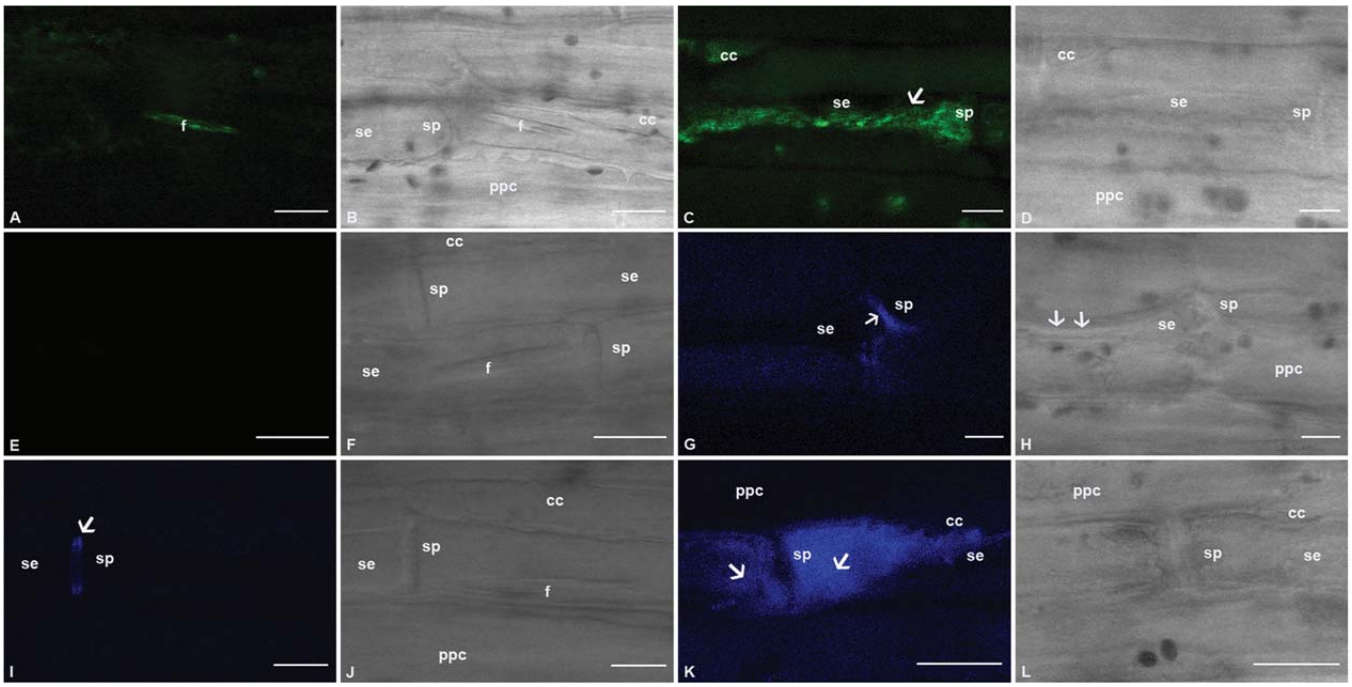

Fig. 3. Confocal laser-scanning microscopy (CLSM) and transmission microscopic images of phloem tissue in intact healthy (left half of the panel) and Flavescence Dorée (FD)-infected (right half) *Vicia faba* plants. Phloem tissue observed **A** and **C,** at 488 nm and **B** and **D,** under transmission light after combined 5-chloromethyl-fluoresceindiacetate and 5-chloromethyl-eosin-diacetate (CMFDA/CMEDA) staining. **A** and **B,** In healthy sieve elements, forisomes occur in the condensed conformation. **C** and **D,** In FD-infected phloem, forisomes bodies are not visible and nonidentified proteinaceous dispersed material is present along the sieve elements (C, arrow). **E** through **L,** Phloem tissue after aniline blue treatment, specific for callose detection in intact sieve tubes, observed **E, G, I,** and **K,** at 405 nm; and **F, H, J,** and **L,** under transmission light. In healthy sieve elements, callose is not detectable (E) or deposited in small amounts at the sieve-plate margins (I, arrow). In infected plants, aniline blue staining indicates large callose depositions along the sieve elements; in particular, in the vicinity of the sieve plates (G) through to plug formation (K, arrows). Note that forisomes are invisible in sieve elements of infected plants. f = forisome, cc = companion cell, se = sieve element, ppc = phloem parenchyma cell, sp = sieve plate. In H, arrows indicate thickened sieve-element walls. Bars correspond to 10 µm.

and co-workers (2004) used CLSM to detect phytoplasmas in freshly sectioned stems and petioles of *Euphorbia pulcherrima* and *C. roseus*. Using two different DNA dyes (SYTO 13 and $DiOC_7(3)$), phytoplasmas appeared as dense fluorescent masses in sieve elements.

All in all, however, involvement of callose as well as proteinaceous substances in plant defense reactions has not been conclusively proven thus far, given the native occlusion reactions in response to sectioning (Knoblauch and van Bel 1998). Computerized image processing and analysis by CLSM using an array of vital fluorescent probes appears to be the appropriate tool for in vivo investigation of phloem-specific phytoplasmas and their interactions with the plant host (Reichel and Beachy 1998). Therefore, we used CLSM techniques for observation of phtytoplasmas in the phloem of intact plants (Knoblauch and van Bel 1998).

Diverse fluorochromes enabled us to stain and distinguish in vivo structural components of intact sieve elements in both intact healthy and FD-diseased *V. faba* plants. The images provided real-time information on structural and biochemical modifications in sieve elements following phytoplasma infection. The DNA-specific dye DAPI was used to detect phytoplasmas in diseased plants (Loi et al. 2002), and identified phytoplasmas inside sieve elements in vivo. Use of DAPI in living cells, as well as the fact that it does not affect cell viability, is well documented in literature for both animal and plant cells (Cai et al. 2008; Ocarino et al. 2008; Subramaniam et al. 2001). Phytoplasmas were found to be distributed along the sieve elements, particularly in the vicinity of the sieve plates. In the enucleate sieve elements (van Bel 2003), no interference with nuclear staining can occur. Theoretically, sieve-element plastids which are of the same size as phytoplasmas may have become stained as well but there is no overlap between the location of the plastids and the DAPI-stained dots.

Phytoplasmas trigger Ca^{2+} influx leading to sieve-element occlusion.

The membrane-permeant, colorless CFDA enters sieve elements via the plasma membrane and, following de-esterification, the membrane-impermeant carboxyfluorescein is translocated by mass flow through the sieve tubes (Oparka et al. 1994). Most of it is retrieved by companion cells and phloem parenchyma cells along the pathway and sequestered in the vacuoles (Knoblauch and van Bel 1998). Its phloem-mobility is indicative of mass flow. In diseased plants, mass flow was significantly reduced compared with the healthy ones and, in most cases, had fully ceased. DAPI/CFDA double staining demonstrated that stoppage of mass flow and phytoplasma accumulation coincide.

Although phytoplasma aggregates may be able to plug the sieve pores, it is more likely that phytoplasma-induced sealants are responsible for sieve-tube occlusion. It is important to underline that CFDA has been detected in the companion cell vacuoles of the diseased plants, indicating that the companion cell activity is not totally impaired by infection, which could be important for phytoplasma survival. After having lost nuclei and most of their organelles during their ontogeny, sieve-elements rely on the metabolic activities of companion cells (van Bel et al. 2002) and may fail to fully nourish phytoplasmas. Companion cells are metabolically active and provide all the compounds essential for sieve-element maintenance. Because phytoplasmas lack many genes indispensable for cell metabolism (Christensen et al. 2005), compounds provided by companion cells might be an important source of nutrition for these pathogens.

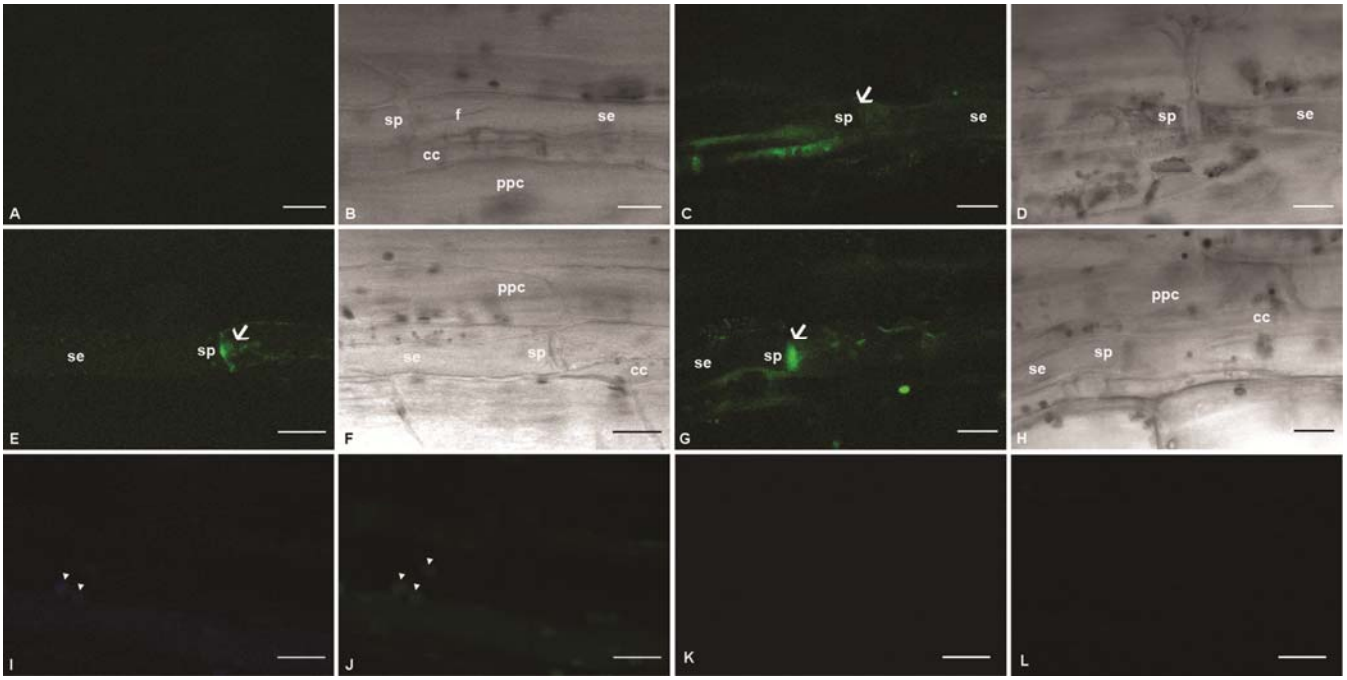

Fig. 4. A through **H,** Confocal laser-scanning microscopy (CLSM) and transmission microscopic images of healthy (left half of the panel) and Flavescence Dorée (FD)-infected (right half) *Vicia faba* phloem after Oregon Green 1,2-bis(o-aminophenoxy)ethane-N,N,-N′,N′-tetraacetic acid (OGB-1) staining, observed **A, C, E,** and **G,** at 488 nm; and **B, D, F,** and **H,** under transmission light. In healthy sieve elements, OGB-1 fluorescence is absent (A) or weakly present in the sieve plate region (E, arrow). In infected plants, the fluorescence signal is very strong along the sieve-element plasma membrane (C), particularly at the sieve plates (G). Note the dark undefined substances in sieve elements of FD-infected plants (D and H) and the transparent sieve elements of healthy plants (B and F). **I** through **L,** CLSM of unstained *Vicia faba* phloem, observed at 405 and 488 nm. Sieve elements of healthy plants using **I,** 405 nm or **J,** 488 nm do not exhibit strong signals. Arrowheads indicate autofluorescence of chloroplasts in the parenchyma cell above the sieve element. Similar results were obtained for FD-infected sieve elements both at **K,** 405-nm and **L,** 488-nm wavelengths. f = forisome, cc = companion cell, se = sieve element, ppc =: phloem parenchyma cell, sp = sieve plate. Bars correspond to 10 µm.

Severe phytoplasma infection is inextricably bound up with forisome dispersion and callose deposition. In FD-diseased plants, spindle-shaped forisomes are dispersed and, hence, become invisible under the light microscope, while high amounts of callose occur in the vicinity of the sieve plates and sometimes in the adjacent zones. Forisome dispersion and callose deposition are Ca^{2+} dependent (Knoblauch et al. 2001; Thonat et al. 1993) and are likely triggered by release of Ca^{2+} into the sieve element lumen (Furch et al. 2009; Hafke et al. 2009). pH-induced modifications in functional (mass flow blockage) and structural (forisome dispersion) properties in FD-infected sieve elements can be excluded. It has been reported that the pH of phloem exudates from phytoplasma-infected plants is not different from that of exudates from control plants (7.5 to 8.0) (Kollar and Seemüller 1990). In addition, forisomes only disperse at nonphysiological pH values under 4 and above 11 (Knoblauch et al. 2003) and, hence, the pH induction of changes in the forisome conformation is more than unlikely.

Application of OGB-1 verified the correlation between phloem occlusion—induced by phytoplasmas—and the rise of Ca^{2+} concentration inside FD-diseased sieve elements (Furch et al. 2007). In diseased plants, the Ca^{2+} concentration in the sieve elements was markedly elevated compared with the healthy ones. The presence of other unidentified protein structures indicates that phloem proteins other than forisomes are involved in sieve-pore plugging in FD-diseased plants, as already shown for cucurbits in response to abiotic stresses and stimuli (Furch et al. 2010).

It appears that phytoplasma infection—possibly by secretion of phytoplasma effectors (Sugio et al. 2011)—induces Ca^{2+} influx into the sieve elements. The scattered distribution of Ca^{2+} ions inside the sieve elements and callose deposition along the longitudinal walls indicates that the phytoplasma effectors activate Ca^{2+} channels not only near the sieve plates but also at other Ca^{2+} hotspots such as the pore-plasmodesma units between sieve elements and companion cells (Furch et al. 2009; Hafke et al. 2009). Recovery of the occlusion phenomena some time after the passage of electrical potential waves demonstrated that occlusion can be reversed following Ca^{2+} extrusion (Furch et al. 2007, 2010). However, it seems that, in FD-diseased broadbean, phytoplasmas impose continuous gating of the Ca^{2+} channels, given the permanent occlusion of infected sieve elements. On the other hand, in some plant–phytoplasma interactions (i.e., apple, alder, and aspen), and in only a few highly susceptible individuals, sealing mechanisms may be considerably affected, leading to sieve-tube sap exudation from cut, infected trunks (Kollar and Seemüller 1990; Kollar et al. 1989).

In addition to sieve-plate occlusion, the sieve-element path may also be narrowed in diseased plants by thickening of the walls, as revealed by CLSM observations. Increased sieve element wall thickness and enhanced total phenolics have been reported for phytoplasma-diseased plants (Choi et al. 2004; Musetti et al. 2000). This would be consistent with apposition of phenolic materials—probably by companion cells, because a Golgi system is absent in sieve elements—against the sieve-element walls for most of those facing the companion cells. It has been demonstrated that a Ca^{2+} signal is required to induce phenylalanine ammonia-lyase (PAL) activity (Messiaen et al. 1993), a key enzyme of the phenol synthesis pathway, as well as PAL gene expression (Long and Jenkins 1998). This would add an interesting side-effect of Ca^{2+} influx on phytoplasma restriction.

In conclusion, we demonstrated that phytoplasma infection leads to sieve-tube occlusion, impairing phloem functions in *V. faba* plants. In systemically infected plants, phytoplasmas—probably by secretion of effector proteins—trigger Ca^{2+} influx into the sieve elements, conferring forisome dispersion, callose deposition, and probably cell wall thickening. The discovery of phytoplasma effector proteins (Sugio et al. 2011) could give a boost to studies of the initial mechanisms involved in phloem–phytoplasma interactions. Application of phytoplasma effectors to intact plants might help to establish the time course of the events involved in phloem reactions to infection.

MATERIALS AND METHODS

Plant material and phytoplasma inoculation.

V. faba plants ('Aguadulce supersimonia') were infected with the phytoplasma related to FD, '*Ca*. P. vitis', strain C (16SrV-C) (Lee et al. 2004). FD-infective leafhoppers (*Euscelidius variegatus*) were caged to inoculate 15-day-old broadbean seedlings in a controlled environment insectarium (22°C, 16-h photoperiod) for a week. Test plants were sprayed with an insecticide solution after the inoculation period and kept in a greenhouse for further growth. The greenhouse conditions were 22 to 25°C (day) and 12 to 16°C (night), 40 to 80% relative humidity, and a 16-h photoperiod. Control plants were not exposed to leafhoppers. FD symptoms (leaf-size reduction along with yellowing and curling) emerged approximately 1 month after inoculation by the vectors.

Phytoplasma presence was assessed by RT-PCR analyses. Total DNA was extracted from 1 g of frozen leaf midribs according to Doyle and Doyle (1990). RT-PCR analyses were performed using the 16S rDNA-based phytoplasma universal primer pair 16S (RT) F1 and 16S (RT) R1, in a DNA Engine Opticon2 System using 40 ng of DNA, 10× PCR buffer, 2.5 mM dNTPs, 25 mM $MgCl_2$, primers at 300 nM each, 0.15 µl of AmpliTaq Gold DNA Polymerase at 5 U/µl (Applied Biosystems, Foster City, CA, U.S.A.) and 10× SYBR Green I in dimethyl sulfoxide (Molecular Probes, Invitrogen, Eugene, OR, U.S.A.) in a total volume of 25 µl. Thermocycling was performed using the following conditions: 11 min at 95°C; 40 cycles of 15 s at 94°C, 15 s at 57°C, and 20 s at 72°C; and 8 min at 72°C. The melting curve was performed with a ramp from 65 to 95°C at 0.2°C/s.

Preparation of intact plants for microscopy.

For in vivo observation of sieve tubes, cortical cell layers were removed from the lower side of the main vein of a fully expanded leaf, still attached to an intact plant, to provide a CLSM observation window (Knoblauch and van Bel 1998). In translocation experiments, phloem-mobile dyes were administered to the cut midrib after having removed the leaf tip at a distance of approximately 3 cm from the observation window. In the other tests, fluorochromes were administered directly on the bare-lying phloem tissues at the observation window. Observations were performed using four healthy and four diseased 6-week-old plants, as soon as symptoms appeared on the infected ones. The experiments were repeated on at least two different leaves per plant.

Fluorescent probes and CLSM imaging.

An apoplasmic physiological buffer containing 1 mM $CaCl_2 \cdot 2H_2O$, 2 mM KCl, 50 mM mannitol, 2.5 mM MES $\cdot H_2O$, and 1 mM $MgCl_2 \cdot 6H_2O$, pH 5.7, was used to solve the dyes (Knoblauch and van Bel 1998). The fluorochromes were imaged by CLSM using a Leica TCS SP2 (Leica Microsystems, Rijswijk, The Netherlands) equipped with a 75-mW argon/krypton laser (Omnichrome, Chino, CA, U.S.A.). Aniline blue and DAPI (Sigma, Milano, Italy) fluorescence was recorded by a Leica TCS SP2 CLSM equipped with a UV laser (Leica Microsystems). The phloem tissue was observed at the observa-

tion window using a ×63 water immersion objective (HCX APO L40x0.80 W U-V-I objective; Leica Microsystems) in the dipping mode.

The phloem-mobile dye CFDA (Invitrogen, Karlsruhe, Germany) was used to investigate phloem flow in healthy and FD-infected plants. After application of drops of a freshly prepared 1 µM CFDA solution followed by an incubation period of 2 h at room temperature, the phloem tissue was examined at 488 nm.

Local staining by DAPI enabled detection of phytoplasmas inside intact sieve elements. A drop of DAPI (1 µg/ml) was applied to the observation window. After incubation for 15 to 20 min at room temperature in darkness, DAPI was removed and replaced by the apoplasmic buffer and the tissue was observed at 405 nm. In the majority of experiments, DAPI and CFDA were applied in succession (or in the reverse order) and the phloem tissue was observed at 405 as well as at 488 nm.

CMEDA/CMFDA mixtures (Molecular Probes), both membrane-permeant fluorochromes, were used for forisome and protein observations in intact sieve tubes, according to Furch and co-workers (2007). Drops of a freshly prepared mixture (1:1, vol/vol) were applied to the observation window and incubated for 1 h at room temperature. Tissues were observed at 488 nm.

In order to visualize callose depositions, a drop of aniline blue, (Merck, Darmstadt, Germany) at the non-lethal concentration of 0.005% (Furch et al. 2007), was applied to the observation window and incubated for 30 min at room temperature. Aniline blue fluorescence was detected at 405 nm.

To reach a qualitative indication of Ca^{2+} concentrations in sieve elements, the membrane-permeant Ca^{2+} marker OGB-1 (Molecular Probes) was applied at a concentration of 5 µM and incubated for 30 min. After removal of dye by rinsing with apoplasmic buffer for 30 min, observations were performed at 488 nm.

To eliminate misinterpretations due to autofluorescence, in vivo unstained *V. faba* sieve elements were observed by CLSM at the same excitation wavelengths used for the above-mentioned fluorochromes (i.e., 488 or 405 nm) as controls.

ACKNOWLEDGMENTS

This work was supported by the Deutscher Akademischer Austauschdienst (DAAD), (grant number A/11/04104 for R. Musetti). R. Musetti and S. V. Buxa contributed equally to this publication. R. Musetti conceived the project under the supervision of A. J. E. van Bel and K.-H. Kogel. S. V. Buxa established the protocols for CLSM. A. Loschi prepared *Vicia faba* infected plants. F. De Marco and R. Polizzotto performed phytoplasma detection by real-time RT-PCR on *V. faba* leaves. R. Musetti and A. J. E. van Bel wrote the manuscript. We thank D. Bosco, Dipartimento di Valorizzazione e Protezione delle Risorse Agroforestali, University of Torino (Italy), for kindly providing infected *Vicia faba* plants; A. Holz and A. Dorresteijn, University of Giessen, for providing a CLSM equipped with a UV laser; and S. Grisan, University of Udine, for expert assistance in preparing the figures.

LITERATURE CITED

Barratt, D. H. P., Kolling, K., Graf, A., Pike, M., Calder, G., Findlay, K., Zeeman, S. C., and Smith, A. M. 2011. Callose synthase GLS7 is necessary for normal phloem transport and inflorescence growth in *Arabidopsis*. Plant Physiol. 155:328-341.

Braun, E. J., and Sinclair, W. A. 1978. Translocation in phloem necrosis-diseased American elm seedlings. Phytopathology 68:1733-1737.

Cai, J., Zhang, X., Wang, X., Li, C., Liu, G. 2008. In vivo MR imaging of magnetically labeled mesenchymal stem cells transplanted into rat liver through hepatic arterial injection. Contrast Media Mol. Imag. 3:72-77.

Choi, Y. H., Casas Tapias, E., Kim, H. K., Lefeber, A. W. M., Erkelens, C., Verhoeven, J. Th. J., Brzin, J., Zel, J., and Verpoorte, R. 2004. Metabolic discrimination of *Catharanthus roseus* leaves infected by phytoplasma using 1H-NMR spectroscopy and multivariate data analysis. Plant Physiol. 135:2398-2410.

Christensen, N. M., Nicolaisen, M., Hansen, M., and Schulz, A. 2004. Distribution of phytoplasmas in infected plants as revealed by real-time PCR and bioimaging. Mol. Plant-Microbe Interact. 17:1175-1184.

Christensen, N. M., Axelsen, K. B., Nicolaisen, M., and Schulz, A. 2005. Phytoplasmas and their interactions with hosts. Trends Plant Sci. 10:526-535.

Cronshaw, J., and Sabnis, D. D. 1990. Phloem proteins. Pages 255-383 in: Sieve Elements. Comparative Structure, Induction and Development. H.-D. Behnke and R. D. Sjolund, eds. Springer-Verlag, Berlin.

Doyle, J. J., and Doyle, J. L. 1990. Isolation of plant DNA from fresh tissue. Focus 12:13-15.

Ehlers, K., Knoblauch, M., and van Bel, A. J. E. 2000. Ultrastructural features of well-preserved and injured sieve elements: Minute clamps keep the phloem transport conduits free for mass flow. Protoplasma 214:80-92.

Elad, Y., and Evensen, K. 1995. Physiological aspects of resistance to *Botrytis cinerea*. Phytopathology 85:637-643.

Faoro, F. 2005. Perché è così difficile osservare al microscopio elettronico i fitoplasmi della vite? Petria 15:99-101.

Furch, A. C. U., Hafke, J. B., Schulz, A., and van Bel, A. J. E. 2007. Ca^{2+}-mediated remote control of reversible sieve tube occlusion in *Vicia faba*. J. Exp. Bot. 58:2827-2838.

Furch, A. C. U., van Bel, A. J. E., Fricker, M. D., Felle, H. H., Fuchs, M., and Hafke, J. B. 2009. Sieve element Ca^{2+} channels as relay stations between remote stimuli and sieve tube occlusion in *Vicia faba*. Plant Cell 21:2118-2132.

Furch, A. C. U., Zimmermann, M. R., Will, T., Hafke, J. B., and van Bel, A. J. E. 2010. Remote-controlled stop of phloem mass flow by biphasic occlusion in *Cucurbita maxima*. J. Exp. Bot. 61:3697-3708.

Goodwin, P. B., Shepherd, V., and Erwee, M. G. 1990. Compartmentation of fluorescent tracers injected into the epidermal cells of *Egeria densa* leaves. Planta 181:129-136.

Hafke, J. B., Furch, A. C. U., Fricker, M. D., and van Bel, A. J. E. 2009. Forisome dispersion in *Vicia faba* is triggered by Ca^{2+} hotspots created by concerted action of diverse Ca^{2+} channels in sieve elements. Plant Signal. Behav. 4:968-972.

Hogenhout, S. A., Oshima, K., Ammar, E., Kakizawa, S., Kingdom, H. N., and Namba, S. 2008. Phytoplasmas: Bacteria that manipulate plants and insects. Mol. Plant Pathol. 9:403-423.

Kartte, S., and Seemüller, E. 1991. Histopathology of apple proliferation in *Malus* taxa and hybrids of different susceptibility. J. Phytopathol. 131:149-160.

Knoblauch, M., and van Bel, A. J. E. 1998. Sieve tubes in action. Plant Cell 10:35-50.

Knoblauch, M., Peters, W. S., Ehlers, K., and van Bel, A. J. E. 2001. Reversible calcium-regulated stopcocks in legume sieve tubes. Plant Cell 13:1221-1230.

Knoblauch, M., Noll, G. A., Müller, T., Prüfer, D., Schneider-Hüther, I., Scharner, D., van Bel, A. J. E., and Peters, W. S. 2003. ATP-independent contractile proteins from plants. Nat. Mater. 2:600-603.

Koh, E.-J., Zhou, L., Williams, D. S., Park, J., Ding, N., Duan, Y.-P., and Kang, B.-H. 2012. Callose deposition in the phloem plasmodesmata and inhibition of phloem transport in citrus leaves infected with '*Candidatus* Liberibacter asiaticus'. Protoplasma 249:687-697.

Köhle, H., Jeblick, W., Poten, F., Blascheck, W., and Kauss, H. 1985. Chitosan-elicited callose synthesis in soybean cells as a Ca^{2+}-dependent process. Plant Physiol. 77:544-551.

Kollar, A., and Seemüller, E. 1990. Chemical composition of phloem exudate of mycoplasma-infected apple trees. J. Phytopathol. 128:99-111.

Kollar, A., Seemüller, E., and Krczal, G. 1989. Impairment of the sieve tube sealing mechanism of trees infected by Mycoplasma-like organisms. J. Phytopathol. 124:7-12.

Lee, I. M., Martini, M., Marcone, C., and Zhu, S. F. 2004. Classification of phytoplasma strains in the elm yellows group (16SrV) and proposal of '*Candidatus* Phytoplasma ulmi' for the phytoplasma associated with elm yellows. Intern. J. Syst. Evol. Microbiol. 54:337-347.

Lepka, P., Stitt, M., Moll, E., and Seemüller, E. 1999. Effect of phytoplasmal infection on concentration and translocation of carbohydrates and amino acids in periwinkle and tobacco. Physiol. Mol. Plant Pathol. 55:59-68.

Lherminier, J., Courtois, M., and Caudwell, A. 1994. Determination of the distribution and multiplication sites of Flavescence Dorée mycoplasma-like organisms in the host plant *Vicia faba* by ELISA and immunocytochemistry. Physiol. Mol. Plant Pathol. 45:125-138.

Lherminier, J., Benhamou, N., Larrue, J., Milet, M. L., Boudon-Padieau, E., Nicole, M., and Blein, J. P. 2003. Cytological characterization of elicitin induced protection in tobacco plants infected by *Phytophthora parasitica* or phytoplasma. Phytopathology 93:1308-1319.

Loi, N., Ermacora, P., Carraro, L., Osler, R., and Chen, T. A. 2002. Production of monoclonal antibodies against apple proliferation phytoplasma and their use in serological detection. Eur. J. Plant Pathol. 108:81-86.

Long, J. C., and Jenkins, G. I. 1998. Involvement of plasma membrane redox activity and calcium homeostasis in the UV-B and UV-A/blue light induction of gene expression in *Arabidopsis*. Plant Cell 10:2077-2086.

Marcone, C. 2010. Movement of phytoplasmas and the development of disease in the plant. Pages 114-131 in: Phytoplasmas: Genomes, Plant Hosts and Vectors. P. Jones and P. Weintraub, eds. CABI Publishing, Wallingford, U.K.

Marcone, C., Neimark, H., Ragozzino, A., Lauer, U., and Seemüller, E. 1999. Chromosome sizes of phytoplasmas composing major phylogenetic groups and subgroups. Phytopathology 89:805-810.

Maust, B. E., Espadas, F., Talavera, C., Aguilar, M., Santamaria, J. M., and Oropeza, C. 2003. Changes in carbohydrate metabolism in coconut palms infected with the lethal yellowing phytoplasma. Phytopathology 93:976-981.

Messiaen, J., Read, N. D., van Cutsem, P., and Trewavas, A. J. 1993. Cell wall oligogalacturonides increase cytosolic free calcium in carrot protoplasts. J. Cell Sci. 104:365-371.

Musetti, R., and Favali, M. A. 1999. Histological and ultrastructural comparative study between *Prunus* varieties of different susceptibility to plum leptonecrosis. Cytobios 99:73-82.

Musetti, R., Favali, M. A., Carraro, L., and Osler, R. 1994. Histological detection of Mycoplasma like organisms causing leptonecrosis in plum trees. Cytobios 78:81-90.

Musetti, R., Favali, M. A., and Pressacco, L. 2000. Histopathology and polyphenol content in plants infected by phytoplasmas. Cytobios 102:133-147.

Musetti, R., Tubaro, F., Polizzotto, R., Ermacora, P., and Osler, R. 2008. Il "Recovery" da Apple Proliferation in melo è associato all' aumento della concentrazione dello ione calcio nel floema. Petria 18:380-383.

Musetti, R., Paolacci, A., Ciaffi, M., Tanzarella, O. A., Polizzotto, R., Tubaro, F., Mizzau, M., Ermacora, P., Badiani, M., and Osler, R. 2010. Phloem cytochemical modification and gene expression following the recovery of apple plants from apple proliferation disease. Phytopathology 100:390-399.

Musetti, R., De Marco, F., Farhan, K., Polizzotto, R., Santi, S., Ermacora, P., and Osler, R. 2011. Phloem-specific protein expression patterns in apple and grapevine during phytoplasma infection and recovery. Bull. Insectol. 64 (Suppl.):211-212.

Ocarino, N. M., Bozzi, A., Pereira, R. D. O., Breyner, N. M., Silva, V. L., Castanheira, P., Goes, A. M., and Serakides, R. 2008. Behavior of mesenchymal stem cells stained with 4′,6-diamidino-2-phenylindole dihydrochloride (DAPI) in osteogenic and non osteogenic cultures. Biocell 32:175-183.

Oparka, K. J., Duckett, C. M., Prior, D. A. M., and Fisher, D. B. 1994. Real-time imaging of the phloem unloading in the root tip of *Arabidopsis*. Plant J. 6:759-766.

Pelissier, H. C., Peters, W. S., Collier, R., van Bel, A. J. E., and Knoblauch, M. 2008. GFP tagging of sieve element occlusion (SEO) proteins results in green fluorescent forisomes. Plant Cell Physiol. 49:1699-1710.

Reichel, C., and Beachy, R. N. 1998 Tobacco mosaic virus infection induces severe morphological changes of the endoplasmic reticulum. Proc. Natl. Acad. Sci. U.S.A. 95:11169-11174.

Rüping, B., Ernst, A.M., Jekat, S. B., Nordzieke, S., Reineke, A. R., Müller, B., Bornberg-Bauer, E., Prüfer, D., and Noll, G. A. 2010. Molecular and phylogenetic characterization of the sieve element occlusion gene family in Fabaceae and non-Fabaceae plants. BMC Plant Biol. 10:219.

Subramaniam, R., Desveaux, D., Spickler, C., Michnick, S. W., and Brisson, N. 2001. Direct visualization of protein interactions in plant cells. Nat. Biotechnol. 19:769-772.

Sugio, A., Kingdom, H. N., MacLean, A. M., Grieve, V. M., and Hogenhout, S. A. 2011. Phytoplasma protein effector SAP11 enhances insect vector reproduction by manipulating plant development and defense hormone biosynthesis. Proc. Natl. Acad. Sci. U.S.A. 108:E1254-E1263.

Thonat, C., Boyer, N., Penel, C., Courduroux, J. C., and Gaspar, T. 1993. Cytological indication of the involvement of calcium and calcium-related proteins in the early responses of *Bryonia dioica* to mechanical stimulus. Protoplasma 176:133-137.

Thorpe, M. R., Furch, A. C. U., Minchin, P. E. H., Föller, J., van Bel, A. J. E., and Hafke, J. B. 2010. Rapid cooling triggers forisome dispersion just before phloem transport stops. Plant Cell Environ. 33:259-271.

Tuteja, N., Umate, P., and van Bel, A. J. E. 2010. Forisomes: Calcium-powered protein complexes with potential as 'smart' biomaterials. Trends Biotechnol. 28:102-110.

Van Bel, A. J. E. 2003. The phloem, a miracle of ingenuity. Plant Cell Environ. 26:125-149.

Van Bel, A. J. E., Ehlers, K., and Knoblauch, M. 2002. Sieve elements caught in the act. Trends Plant Sci. 7:126-132.

Xie, B., Wang, X., Zhu, M., Zhang, Z., and Hong, Z. 2011. *CalS7* encodes a callose synthase responsible for callose deposition in the phloem. Plant J. 65:1-14.